Supporting Information

Vanadium incorporation in ferrite nanoparticles serves as electron buffer and anisotropy tuner in catalytic activity and hyperthermia applications

T.E.Torres[1,2,3,4†*], D. P. Valdés[5,6*], Simon Hettler[1,2,3], J.M. Nuñez[1,3,5], Irati Rodrigo[7], Iñaki Orue[8], J.Á. Garcia[9], F. Plazaola[10], R. D. Zysler[5,6], E. Lima Jr.[5], M. H. Aguirre[1,2,3], G. F. Goya[1,2] and Raul Arenal[1,2,3,11]

[1] Instituto de Nanociencia y Materiales de Aragón (INMA), CSIC- Universidad de Zaragoza, 50018 Zaragoza, Spain.
[2] Departamento de Física de la Materia Condensada, Facultad de Ciencias Universidad de Zaragoza, 50018, Zaragoza, Spain
[3] Laboratorio de Microscopías Avanzadas (LMA), Universidad de Zaragoza, Calle Mariano Esquillor, 50018, Zaragoza, Spain
[4] Department of Chemistry and Chemical Biology, Rutgers, The State University of New Jersey, 123 Bevier Road, Piscataway, 08854, NJ, USA
[5] Instituto de Nanociencia y Nanotecnología CNEA-CONICET, Av. E. Bustillo 9500, 8400, S. C. Bariloche, RN, Argentina.
[6] Instituto Balseiro, UNCUYO, Av. E. Bustillo 9500, 8400, S.C. Bariloche, RN, Argentina
[7] Departamento Física Aplicada, Universidad del País Vasco (UPV/EHU), Eibar 20600, Spain
[8] SGIker, Universidad del País Vasco – UPV/EHU, 48940 Leioa, Spain
[9] Departamento Física Aplicada, Universidad del País Vasco (UPV/EHU), Leioa 48940, Spain
[10] Departamento de Electricidad y Electrónica, Universidad del País Vasco (UPV/EHU), Leioa 48940, Spain
[11] ARAID Foundation, 50018, Zaragoza, Spain

[*] Corresponding authors: teobaldotorresmolina@gmail.com; daniela.valdes@ib.edu.ar

[†] Previous address: Instituto de Nanociencia y Nanotecnología CNEA-CONICET, Av. E. Bustillo 9500, 8400, S. C. Bariloche, RN, Argentina.

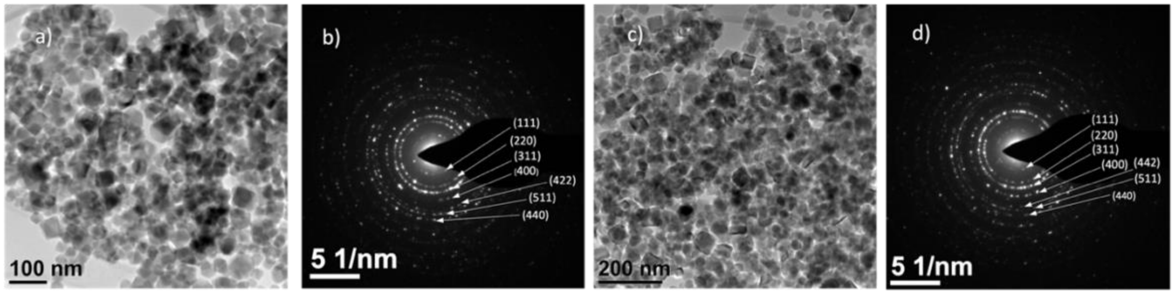

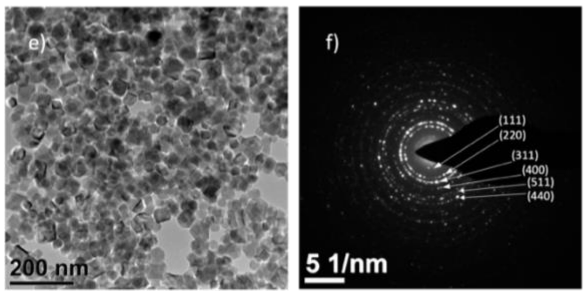

Figure S1. a), c) and e). TEM images of the MNPs. b), d) and f) Their corresponding indexed selected-area electron diffraction patterns for an FCC structure.

Table S1. Interplanar distances for plane families of the FCC structure and the lattice parameter obtained from the images in Figure S1 through the expression a = d_{hkl} $\sqrt{h^2+k^2+l^2}$, yielding the average <a> = (8,60 ± 0,09) Å.

Theoretical Values FCC structure			Experimental values image b)					
<hkl>	$\sqrt{(h^2+k^2+l^2)}$.	g_{hkl}/g_{111}	$1/D_{hkl}$ (nm^{-1})	$1/r_{hkl}$ (nm^{-1})	g_{hkl}/g_{111}	d_{hkl} (nm)	d_{hkl} (Å)	a_{hkl} (Å)
111	$\sqrt{3}=1{,}7321$	1	4,015	2,0075	1	0,4981	4,9813	8,6278
220	$\sqrt{8}=2{,}8284$	1,6329	6,533	3,2665	1,6271	0,3061	3,0613	8,6588
311	$\sqrt{11}=3{,}3166$	1,91478	7,708	3,854	1,9198	0,2594	2,5947	8,6056
400	4	2,3093	9,331	4,6655	2,3240	0,2143	2,1433	8,5735
422	$\sqrt{24}$=4,8989	2,8283	11,304	5,652	2,8154	0,1769	1,7692	8,6676
511	$\sqrt{27}$=5,1962	2,9999	12,171	6,0855	3,0313	0,1643	1,6432	8,5385
440	$\sqrt{32}$=5,6568	3,2658	13,136	6,568	3,2717	0,1522	1,5225	8,6127

Theoretical Values FCC structure			Experimental values image d)					
<hkl>	$\sqrt{(h^2+k^2+l^2)}$.	g_{hkl}/g_{111}	$1/D_{hkl}$ (nm^{-1})	$1/r_{hkl}$ (nm^{-1})	g_{hkl}/g_{111}	d_{hkl} (nm)	d_{hkl} (Å)	a_{hkl} (Å)
111	$\sqrt{3}=1{,}7321$	1	4,086	2,043	1	0,4894	4,8947	8,4779
220	$\sqrt{8}=2{,}8284$	1,6329	6,591	3,2955	1,6130	0,3034	3,0344	8,5826
311	$\sqrt{11}=3{,}3166$	1,91478	7,739	3,8695	1,8940	0,2584	2,5843	8,5711
400	4	2,3093	9,404	4,702	2,3015	0,2126	2,1267	8,5070
422	$\sqrt{24}$=4,8989	2,8283	11,370	5,687	2,7836	0,1758	1,7584	8,6143
511	$\sqrt{27}$=5,1962	2,9999	12,147	6,0735	2,9728	0,1646	1,6464	8,5554
440	$\sqrt{32}$=5,6568	3,2658	13,196	6,598	3,2295	0,1515	1,5156	8,5735

Theoretical Values FCC structure			Experimental values image f)					
<hkl>	$\sqrt{(h^2+k^2+l^2)}$.	g_{hkl}/g_{111}	$1/D_{hkl}$ (nm^{-1})	$1/r_{hkl}$ (nm^{-1})	g_{hkl}/g_{111}	d_{hkl} (nm)	d_{hkl} (Å)	a_{hkl} (Å)
111	$\sqrt{3}=1{,}7321$	1	3,898	1,949	1	0,5130	5,1308	8,8868
220	$\sqrt{8}=2{,}8284$	1,6329	6,538	3,269	1,6271	0,3059	3,0590	8,6522
311	$\sqrt{11}=3{,}3166$	1,91478	7,778	3,889	1,9198	0,2571	2,5713	8,5282
400	4	2,3093	9,408	4,704	2,3240	0,2125	2,1258	8,5034
511	$\sqrt{27}$=5,1962	2,9999	12,065	6,0325	2,8154	0,1657	1,6576	8,6135
440	$\sqrt{32}$=5,6568	3,2658	13,199	6,5995	3,3860	0,1515	1,5152	8,5715

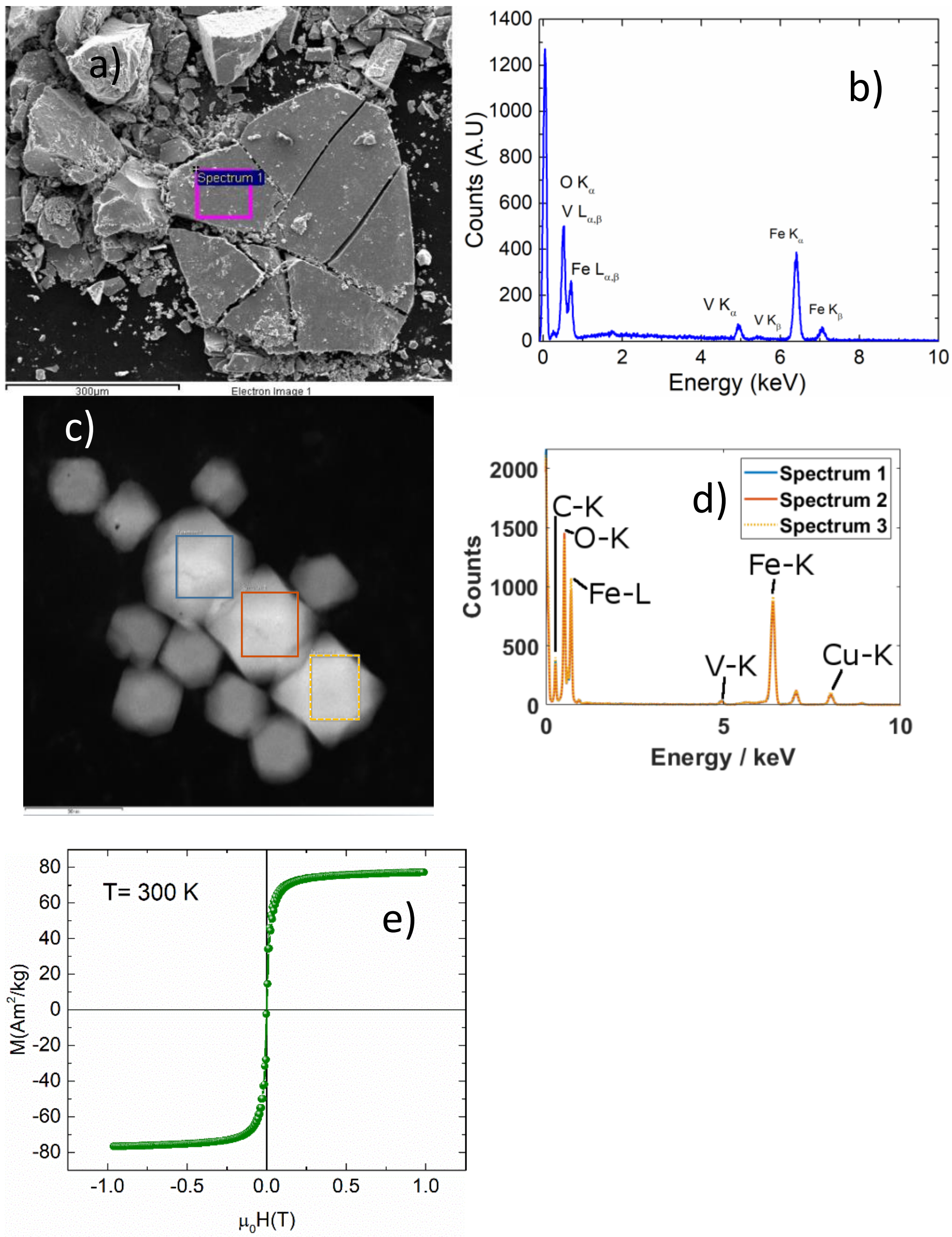

Figure S2. (a) A characteristic SEM image shown one region where the EDX spectra was performed. (b) EDX spectra corresponding the rectangle shown in (a) for a powder sample. (c) STEM imagen shown a series of individual particles. (d) EDX spectra of individual particles corresponding of the rectangles shown in (c). (e) Hysteresis loop a T = 300K and DC conditions.

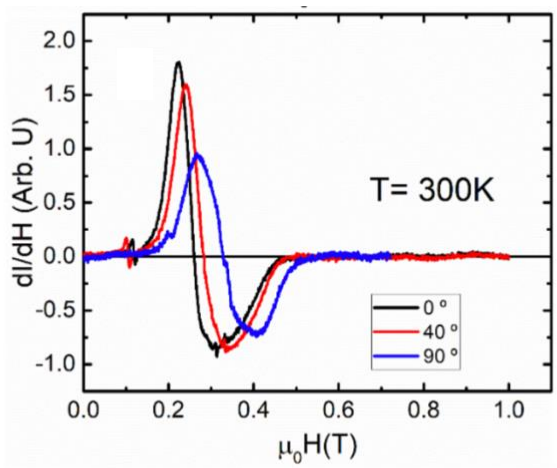

Figure S3. FMR spectra at T = 300 K for different orientations between the external field and the MNPs.

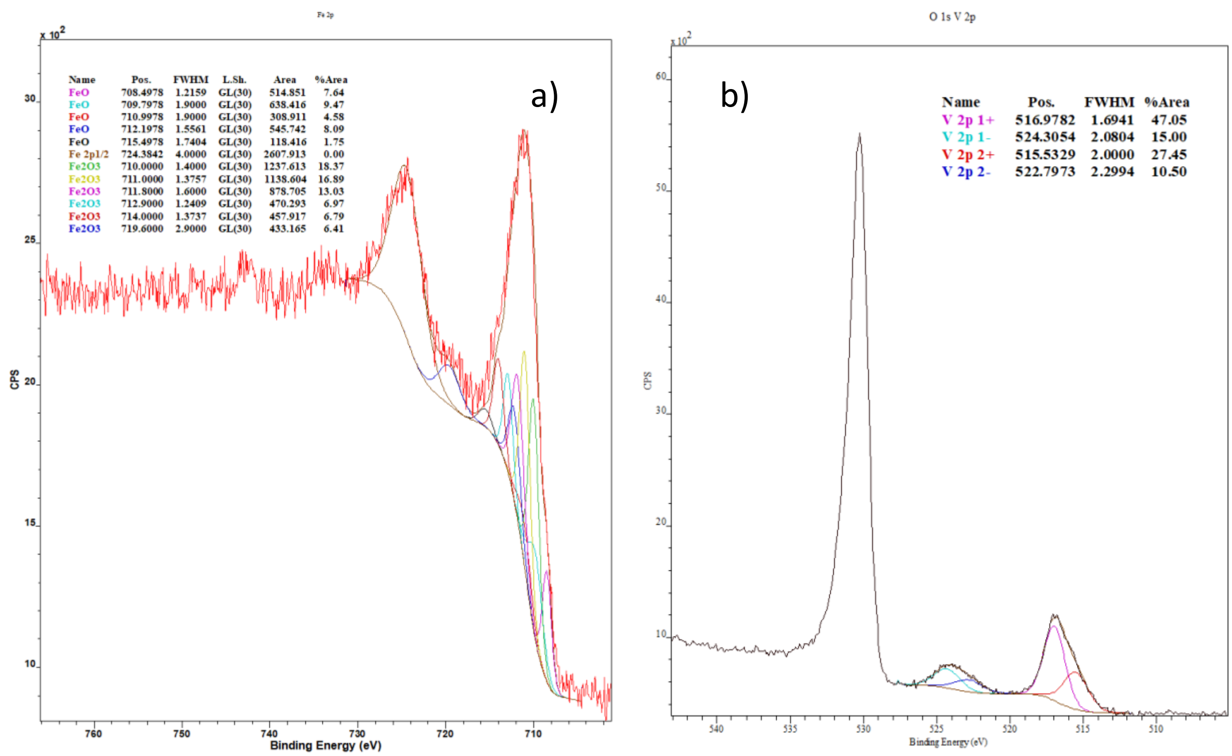

Figure S4. XPS Analysis with the corresponding quantification obtained with the commercial CasaXPS software. (a) Fe edge and (b) V edge.

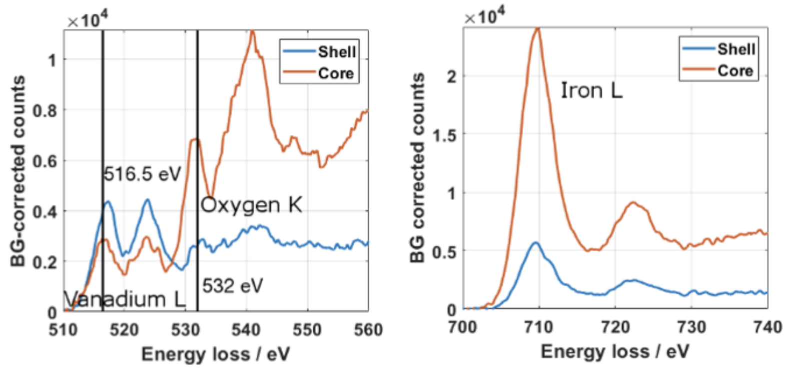

Figure S5. EELS analysis of the (a) O-K and V-L and (b) Fe-L edge taken from the core (red) and V-rich shell region (blue), respectively. The increase in intensity in the V-L edge in the shell is clear, accompanied by a decrease in Fe and O. The V-L double peak slightly sharpens and shifts to higher energy in the shell. The pre-peak of the O-K edge at 532 eV typical for magnetite disappears in the shell. The doublet of the Fe-L3 edge is more clearly seen in the shell, linked to a small increase in intensity of the higher-energy contribution.

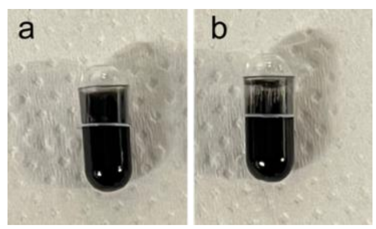

Figure S6. Polyacrylamide gels (a) dispersed and (b) oriented at 0.5 wt% in MNPs

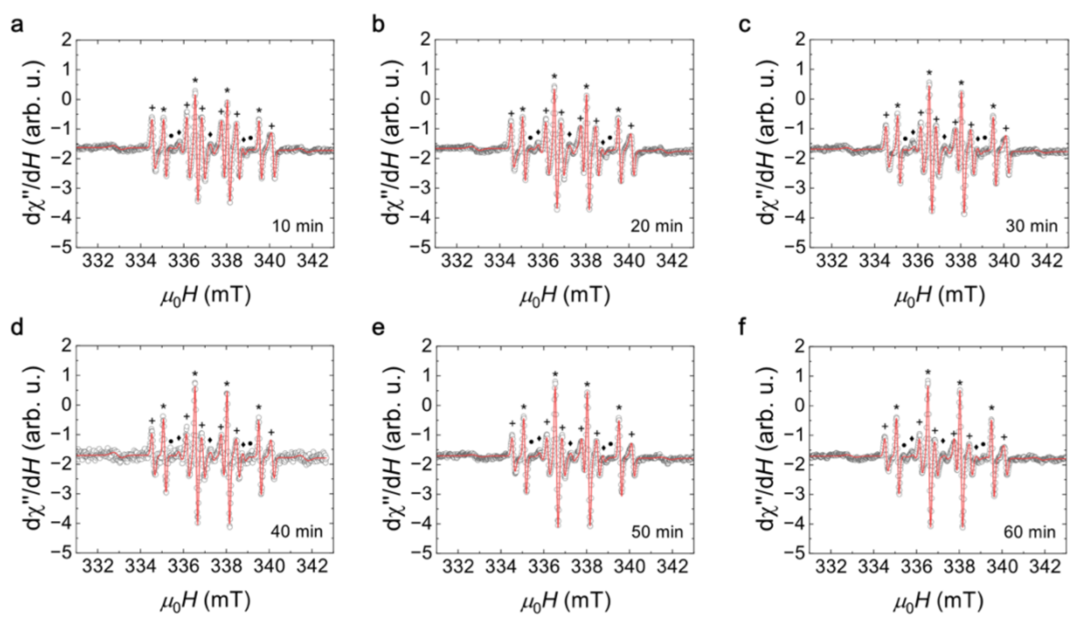

Figure S7. Series of EPR spectra in function of time shown the evolution of radical production.

Table S2. Parameters obtained from the fittings of the EPR spectra for V ferrite MNPs catalytic activity at different times. g = gyromagnetic ratio, L_w= line width, A_{hf} first line is the hyperfine coupling field, second and third line is the hyperfine coupling field between the electronic spin and the nuclear spins of N and H in DMPO/DMSO, respectively.

t (min)		**Mn^{2+}**	**OH**	**CH_3 - a**	**CH_3 - b**	**OOH**	**N**
10	g	1.9984	2.00353	2.00339	2.00333	2.00217	2.00362
	L_w (mT)	0.40006	0.122031	0.178805	0.1347	0.147055	0.166492
	I	0.00196762	0.00292	0.00205	0.00272	0.000197	0.000464
	A_{hf} (MHz)	243.247					40.6611
			41.9002	44.0192	45.7223	40.5382	
			40.8938	63.4193	65.4329	34.2081/4.96593	
20	g	1.99832	2.00352	2.00337	2.00333	2.00298	2.00361
	L_w (mT)	0.394375	0.123842	0.191203	0.136402	0.114785	0.171746
	I	0.00196243	0.00333	0.00179	0.00248	0.000146	0.00042
	A_{hf} (MHz)	245.158					40.9217
			41.8461	44.0142	45.7358	39.6862	
			40.9702	63.5109	65.2937	33.9813/5.22085	
30	g	1.99801	2.00352	2.00339	2.00333	2.00296	2.00333
	L_w (mT)	0.427329	0.122546	0.178805	0.1347	0.0982284	0.179182
	I	0.00178728	0.00367	0.00205	0.00272	0.000155	0.000378
	A_{hf} (MHz)	246.762					41.0769
			41.877	44.0192	45.7223	40.5382	
			40.9641	63.4193	65.4329	34.2081/3.73425	
40	g	1.99743	2.00207	2.00193	2.00188	2.00212	2.0021
	L_w (mT)	0.415736	0.126776	0.156665	0.133578	0.129968	0.183491
	I	0.00459339	0.00532	0.00134	0.00119	0.000183	0.000361
	A_{hf} (MHz)	244.026					41.683
			41.6604	44.7993	45.1613	40.2538	
			40.1141	62.7288	65.9273	33.5759/5.09143	
50	g	1.9974	2.00207	2.00192	2.00188	2.00211	2.0021
	L_w (mT)	0.405302	0.128287	0.155912	0.136111	0.14882	0.180607
	I	0.00365615	0.00535	0.00115	0.00127	0.000216	0.000286
	A_{hf} (MHz)	244.092					41.3172
			41.6318	44.8177	45.1484	40.4201	
			40.0938	62.5034	65.9108	33.5158/5.60089	
60	g	1.99749	2.00207	2.00194	2.00188	2.00192	2.00221
	L_w (mT)	0.434118	0.127648	0.173751	0.127151	0.145432	0.180237
	I	0.00519223	0.00512	0.00138	0.000892	0.000292	0.000198
	A_{hf} (MHz)	243.361					41.9141
			41.646	44.9286	45.1564	39.8784	
			40.1113	62.694	65.9208	33.2591/4.92328	

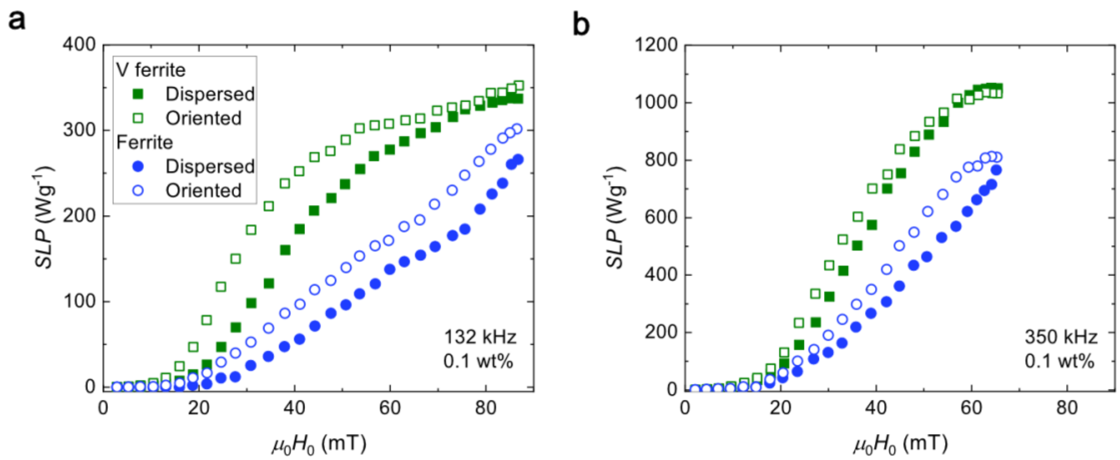

Figure S8. Comparison between *SLP* values for ferrite and V ferrite MNPs dispersed and oriented in polyacrylamide gels, for measurements at (a) 132 and (b) 350 kHz at a MNP concentration of 0.1 wt%.

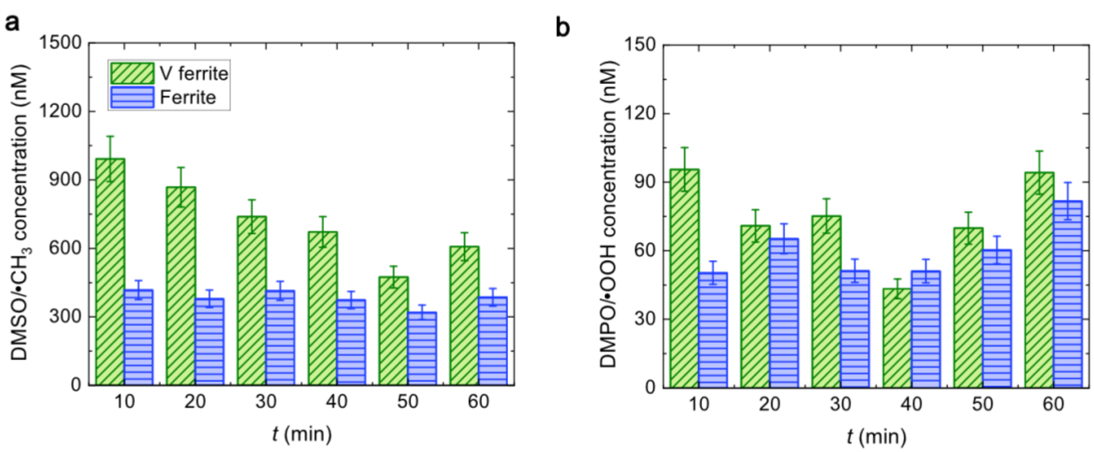

Figure S9. DMSO/CH_3 and DMPO/OOH adduct concentration as a function of time after addition of H_2O_2 for ferrite and V ferrite MNPs in DMPO/DMSO.

Table S3. Parameters obtained from the fittings of the EPR spectra for ferrite MNPs catalytic activity at different times. g = gyromagnetic ratio, L_w= line width, A_{hf} first line is the hyperfine coupling field, second and third line is the hyperfine coupling field between the electronic spin and the nuclear spins of N and H in DMPO/DMSO, respectively.

t (min)		**Mn^{2+}**	**OH**	**CH_3 - a**	**CH_3 - b**	**OOH**	**N**
10	g	1.99740	2.00207	2.00195	2.00186	2.00208	2.00211
	L_w (mT)	0.413419	0.125728	0.1511	0.136917	0.143188	0.182815
	I	0.00460856	0.0038	0.00149	0.00139	0.00018	0.00042
	A_{hf} (MHz)	243.316					41.53
			41.6612	44.7776	45.213	39.9815	
			40.1136	62.9886	66.0404	33.4485/5.687	
20	g	1.99747	2.00207	2.00193	2.00187	2.00203	2.0021
	L_w (mT)	0.420748	0.125783	0.159287	0.136384	0.139471	0.184476
	I	0.00431423	0.0039	0.00136	0.00122	0.000234	0.000306
	A_{hf} (MHz)	243.749					41.5847
			41.877	44.7002	45.1253	40.3709	
			40.119	62.8541	65.8553	33.3348/5.09964	
30	g	1.99751	2.00207	2.00193	2.00187	2.00187	2.00218
	L_w (mT)	0.408448	0.124441	0.15276	0.138361	0.18574	0.169078
	I	0.00443176	0.00513	0.00148	0.00144523	0.00129	0.000183
	A_{hf} (MHz)	243.551					41.6441
			41.6368	44.5988	45.1423	40.3075	
			40.1486	62.9308	65.9282	33.7263/5.24881	
40	g	1.99828	2.00352	2.00338	2.00333	2.0029	2.00355
	L_w (mT)	0.390776	0.116577	0.146979	0.132372	0.119201	0.160597
	I	0.00299142	0.00379	0.00139	0.00203	8.94e-05	0.000387
	A_{hf} (MHz)	243.158					41.6351
			41.8499	45.2512	45.3858	40.3584	
			40.9891	63.0417	66.3008	33.6747/5.33128	
50	g	1.99801	2.00352	2.00334	2.00333	2.00336	2.00356
	L_w (mT)	0.470289	0.122954	0.193003	0.139157	0.176404	0.167013
	I	0.0017901	0.00435	0.000979	0.0023	0.000144	0.000399
	A_{hf} (MHz)	246.927					40.9156
			41.8758	44.113	45.6084	41.4923	
			40.885	63.6066	65.3608	32.0665/3.86795	
60	g	1.99785	2.00353	2.00337	2.00333	2.0031	2.00329
	L_w (mT)	0.424706	0.122445	0.142766	0.130225	0.126337	0.161883
	I	0.00176325	0.00472	0.00125	0.00192	0.000194	0.000189
	A_{hf} (MHz)	244.77					41.586
			41.8718	45.2368	45.4648	40.0255	
			40.9177	62.268	66.4019	33.3552/5.30484	